Numerical Simulation and Experiment for Underwater Shock Wave in Newly Designed Pressure Vessel

Manabu SHIBUTA* , **Hideki HAMASHIMA** ** , **Shigeru ITOH*****
*Graduate School of Science and Technology, Kumamoto Univ.

2-39-1 Kurokami, Kumamoto 860-8555, Japan
manabu@shock.smrc.kumamoto-u.ac.jp
**Kumamoto Industrial Research Institute.
3-11-38 Higashimachi, Kumamoto 862-0901, Japan
hamashima@kmt-iri.go.jp
*** Shock Wave and Condensed Matter Research Center,
Kumamoto Univ.
2-39-1 Kurokami, Kumamoto 860-8555, Japan
itoh@mech.kumamoto-u.ac.jp

ABSTRACT

Modern eating habits depend in large part on the development of food processing technology. Thermal treatments are often performed in the conventional food processing, but it can cause discoloration and loss of nutrients of the food by thermal processing or treatment. On the other hand, food processing using an underwater shock wave has little influence of heat and its processing time is very short, preventing the loss of nutrients. In this research optical observation experiment and the numerical simulation were performed, in order to understand and control the behavior of the underwater shock wave in the development of the processing container using an underwater shock wave for the factory and home. In this experiment a rectangular container was used to observe the behavior of the underwater shock wave. In the experiment, the shock wave was generated by using explosive on the shock wave generation side. The shock wave, which passed through the phosphor bronze and propagated from the aluminum sidewall, was observed on the processing container side. Numerical simulation of an analogous experimental model was investigated, where LS-DYNA software was used for the numerical simulation. The comparative study of the experiment and the numerical simulation was investigated. The behavior of a precursor shock wave from the device wall was able to be clarified. This result is used for development of the device in numerical simulation.

1. INTRODUCTION

Various processing methods of using shock waves generated by explosive and electric power have been studied and developed. It is well established that shock wave pressure propagates on a large range and duration of pulse can be long, depending on the processing techniques. Using water as the propagation medium, the influence of thermal effect can be minimized. However, in the processing techniques using underwater shock wave, it is difficult to control the underwater shock waves.

In this research, an attempt was made to obtain the velocity of the precursor shock wave, shock wave and reflected shock wave. The precursor shock wave propagating through aluminum alloy and underwater shock wave are analyzed in order to understand the behavior of underwater shock wave in the development of the pressure vessel. A high speed camera was used for optical observation of shock waves. And numerical simulation was performed to investigate the validity of data, and these results were compared with experimental results.

2. SHOCK WAVE [1]

Because it is needed in order to determine a boundary and contact conditions in numerical simulation, propagation and reflection of a shock wave are described. If the characteristic of a shock wave is known, it is possible to use suitable conditions in numerical simulation. In this research, propagation of the shock wave between water and a metal plate is investigated. Therefore, the basic characteristic of a shock wave and the action of the incident and reflected wave in a On a boundary surface are explained.

2.1 ABOUT A SHOCK WAVE

The shock wave is a wave of the pressure spread exceeding the sound velocity. It appears when energy is accumulated very short time and released momentarily.

The shock wave can be observed in various places also in everyday life. For example, the shock wave occurs by the tip of the airplane which flies at supersonic velocity, and stabbing with a needle the balloon blown up greatly and a roll of thunder and etc.

2.2 THEORY OF THE SHOCK WAVE

The shock wave phenomenon is one of the most fundamental phenomena produced by the result of density change of the gas treated as compressible fluid. In the dynamics of compressive fluid, the flow of the high-speed gas in consideration of density change and wave motion propagation in gas is dealt with. On the other hand, the liquid and the solid are treated as incompressible fluid. These are not usually accompanied by density change. But if a shock strong against these is given, these will unite immediately and a shock wave will be formed by a compressional wave occurring by interference with the medium. In this time, liquid and solid show the action of compressible fluid.

Therefore, although theory of a shock wave is based on the dynamics of compressible fluid, as for the medium, both the liquid and the solid become the object as well as gas.

If a minute pressure change (turbulence) takes place into stationary gas, this pressure change will be propagated at the sound velocity c. Following equation is formed when the pressure of stationary gas is set as p, density is set as ρ, change of pressure is set as dp, density change to change of pressure is set as $d\rho$, and the velocity of the flow of the gas with the pressure change is set as w.

$$c = \sqrt{\frac{dp}{d\rho}} \tag{2.1.}$$

$$cd\rho = \rho w \tag{2.2.}$$

$$dp = \rho cw \tag{2.3.}$$

It is thought that a large pressure change integrated with a minute pressure change from these formulas. But as shown in a formula (2.2) and (2.3), the individual pressure change will be transmitted in the gas which was able to give velocity w with front pressure. Therefore, it is $w > 0$ from $dp > 0$ and $d\rho > 0$ in the compressional wave, the density gradient in a wave face increases gradually. However, since real gas has viscosity and thermal conductivity, the pressure slope of a compression wave does not become infinite. Therefore, if a change of state reaches a limit, a wave keeps progressing with fixed velocity while keeping the fixed shape. This wave is a shock wave and always a longitudinal wave. And it is considered the wave as pressure changes in the space like a sound wave. Propagation velocity of a shock U_s wave is

$$U_s = c_0 + su_p \tag{2.4.}$$

where u_p is the particle velocity of a medium. It is known experimentally that this linear relation is formed. c_0, s is a constant number and has become clear experimentally about many substances.

If the first pressure change is large, the front of a compression wave will become precipitous, will turn into a discontinuous surface, and will form a shock wave surface. But the formed shock wave surface is stable and propagates without the form changing if disorder by friction from the external world does not enter. It is presupposed that the thickness of a shock wave surface is fixed and form does not change and considered that the state of the front and back of a wave surface. Fig. 1 shows the one-dimensional compression by the plane shock wave which spreads the inside of compressible fluid in the state of a one-dimensional constant. Quantity of state of shock compression before and after is shown by

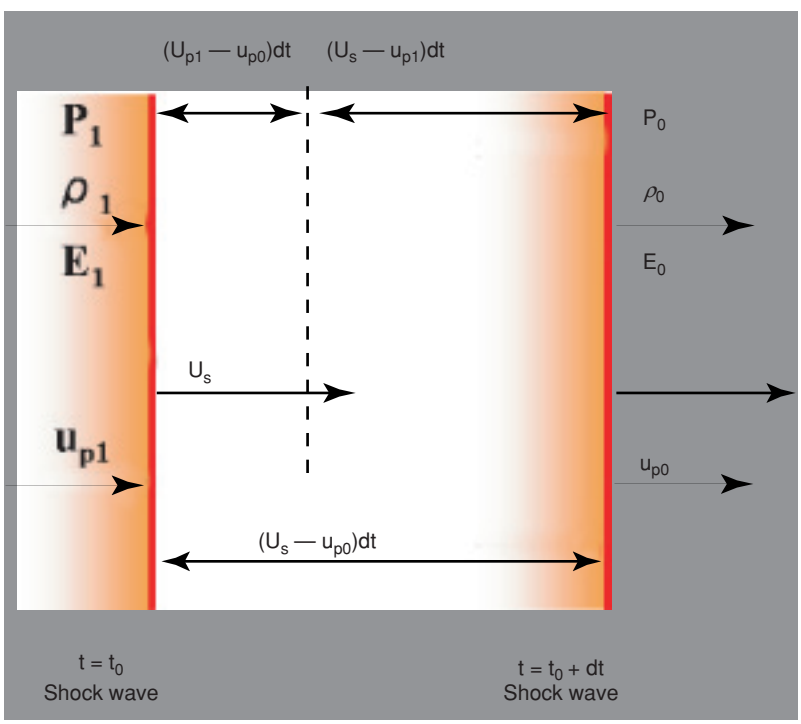

Fig.1 1-dimensional compression by the plane shock wave.

the lower subscripts 0 and 1. In this time, the case where a shock wave propagates the inside of the medium of the particle velocity u_{p0} at velocity U_s during time T, and particle velocity accelerates to u_{p1} is considered. At this time, a shock wave surface propagates only the distance of $(U_s - u_{p0})dt$ and the mass which a wave face crosses to per unit volume is $\rho_0(U_s - u_{p0})dt$.

The medium particle in the back of the wave front become u_{p1}, and to be compressed, the mass crossed per unit volume become $\rho_1(U_s - u_{p1})dt$. The following formula will be obtained if the law of conservation of mass is formed in shock wave surface of the front and back.

$$\rho_0(U_s - u_{p0}) = \rho_1(U_s - u_{p1}) \tag{2.5.}$$

The change in momentum is $\rho_0(U_s - u_{p0})dt \cdot (u_{p1} - u_{p0})$ in shock wave surface of the front and back. Since this change in momentum is equal to impulse $(P_1 - P_0)dt$ acting on the unit area of the wave surface, the following formula consists of momentum conservation law.

$$P_1 - P_0 = \rho_0(U_s - u_{p0})(u_{p1} - u_{p0}) \tag{2.6.}$$

On the other hand, since the work $P_1(u_{p1} - u_{p0})dt$ formed out of pressure P_1 is equal to the sum of the increase $\frac{1}{2}(u_{p1} - u_{p0})^2$ in kinetic energy about the mass $\rho_1(U_s - u_{p0})dt$ which crosses a wave surface per unit area, and the increase $E_1 - E_0$ in internal energy, the following formula consists of conservation law of energy.

$$P_1(u_{p1} - u_{p0}) = \frac{1}{2}\rho_0(U_s - u_{p0})(u_{p1} - u_{p0})^2 + \rho_0(U_s - u_{p0})(E_1 - E_0) \tag{2.7.}$$

If this formula and formula (2.6) and (2.7) are combined, the formula of Rankine-Hugoniot shown below will be obtained.

$$E_1 - E_0 = \frac{1}{2}(P_1 + P_0)(V_0 - V_1) \tag{2.8.}$$

In this point, V is specific volume and is $\frac{1}{\rho}$.

2.3 REFLECTION OF A SHOCK WAVE

2.3.1 The phenomenon in a boundary surface with the different kind medium

When it arrives at the boundary surface of a different kind medium having the property with different character from the medium which a shock wave is propagating, a part of shock wave reflect, and another part transmit and propagate to the different kind medium in this boundary surface.

The characteristic value of the reflected shock wave in a border plane is chosen equation of state like a Gruneisen type, and it is determined according to supposition of either shock compression or adiabatic expansion. In this paper, only the easiest impedance matching method is described.

2.3.2 Impedance matching

When a shock wave transmits to a different material of the shock impedance, two kinds of waves, the transmitted wave spread over a substance and the reflected wave are generated on a boundary surface. The situation is shown in Fig.2. Generally, when the wave incidents into a substance with large shocking impedance, a reflected wave turns into a rarefaction wave, and when the wave incidents into a substance with small shocking impedance, a reflected wave turns into a shock wave.

In this time, the case where the shock wave spread through substance A incidents into Substance B perpendicularly to a boundary surface is considered (Fig. 3(a)). The incident

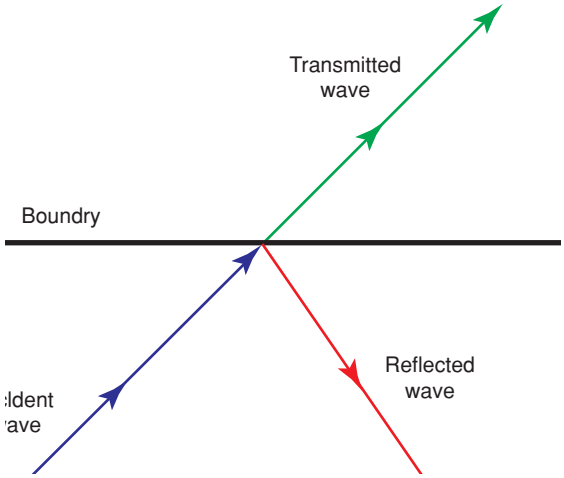

Fig.2 Schematic illustration for reflection of a shock wave.

shock wave is advancing perpendicularly toward a boundary surface at the velocity of U_s^i. When this incident shock wave reflects at a boundary surface, the incident wave is divided into the reflected wave which propagates the inside of Substance A ,and the transmitted wave which is transmitting Substance B (Fig. 3(b)).

It is adapted for an incident wave and a transmitted wave in a law of conservation of momentum of (2.6).

$$P^i - P_0 = \rho_A U_s^i u_p^i \tag{2.9}$$

$$P^t - P_0 = \rho_B U_s^t u_p^t \tag{2.10}$$

Subscript i, t, and r express the incident shock wave, the transmitted wave, and a reflected wave, respectively. ρ_A, ρ_B are taken as each initial density of Substance A and Substance B.

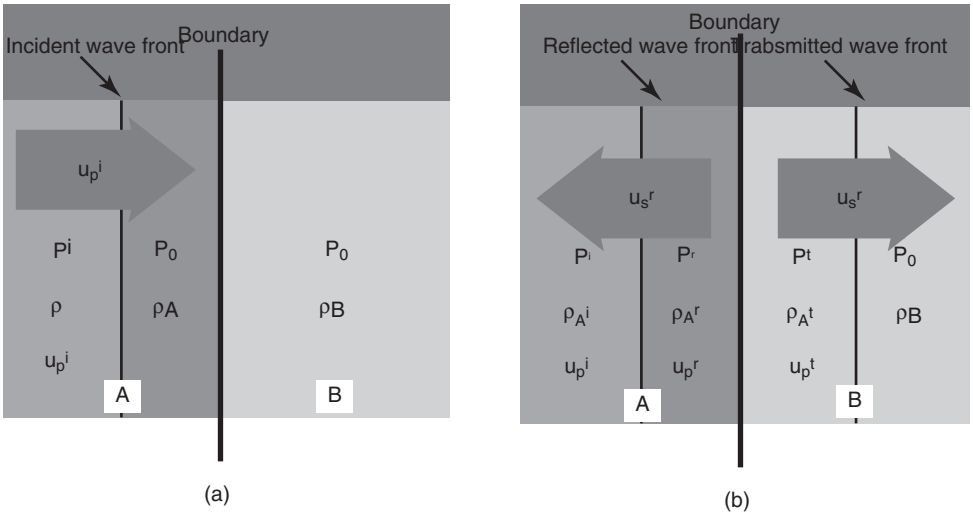

Fig.3 Schematic illustration for incidence, reflection, and transmission of a shock wave in different media.

In this case, it is assumed that the theory of the shock wave is applicable also in the case of a rarefaction wave.

If shock impedance is decided for incident pressure in (2.9) and (2.10), since the incident shock impedance $\rho A U_s^i$ and the reflected shock impedance $\rho A U_s^r$ are equal, the following formula is obtained.

$$\rho_A U_s^i = \rho_A^r U_s^r \tag{2.11}$$

As a result, a law of conservation of momentum is the following formula from Fig.3(b) to a reflected wave.

$$P^r - P^i = \rho_A^r U_s^r (u_p^r - u_p^i) = \rho_A U_S^i (u_p^r - u_p^i) \tag{2.12}$$

As for the reflected pressure P^r and the particle speed u_p^r of the reflected wave back, the following formula is obtained from assumption of continuation.

$$P^t = P^r, u_p^t = u_p^r \tag{2.13}$$

The pressure of a transmitted shock wave in B is the next formula similarly.

$$P^t = \rho_0^B U_s^t u_p^t = \rho_0^B (c^B + s^B u_p^t) u_p^t \tag{2.14}$$

P^r and u_p^r are the following formulas when P_0 is disregarded, since P_0 is very small compared with P^i or P^t and formula from (2.9) to (2.14) .

$$P^r = P^t = \frac{2\rho_B U_s^t}{\rho_A U_s^i + \rho_B U_s^t} P^i \tag{2.15}$$

$$u_p^r = \frac{2\rho_A U_s^i}{\rho_A U_s^i + \rho_B U_s^t} u_p^i \tag{2.16}$$

In use of this impedance matching method, it must be cautious of an error becoming large, so that the pressure difference of an incident wave and a reflected wave and the difference of impedance are large. In the case of a reflected wave is a shock wave, the result of this formula is mostly in agreement. However, in the case of a reflected wave is a rarefaction wave, the result of this formula is not completely in agreement.

2. EXPERIMENTAL METHOD AND NUMERICAL SIMULATION

2.1 OPTICAL OBSERVATION AND MEASUREMENT OF SHOCK WAVE VELOCITY

The optical observation that uses the shadowgraph method [2] was used to evaluate the shock wave propagating. The shadowgraph system used in this study is shown in Fig.4. This system uses a technique, also called direct projective technique, in which the shadow of the light observed and projected by density change on a screen. The shadowgraph method used for visualization of a shock wave or the motion of a wave is a classical technique.

The shadowgraph system and a high-speed video camera (HPV-1:Shimadzu Corp.) were used to observe the underwater shock wave and shock wave propagating in aluminum alloy sidewall.

The velocity of a shock wave is obtained by taking a framing photography using the shadowgraph method. The schematic illustration of an optical observation for the framing photography is shown in Fig.5.

An experimental device is a rectangular container. The observation side of the device is PMMA, the side of the device is aluminum and the upper surface and the bottom of the

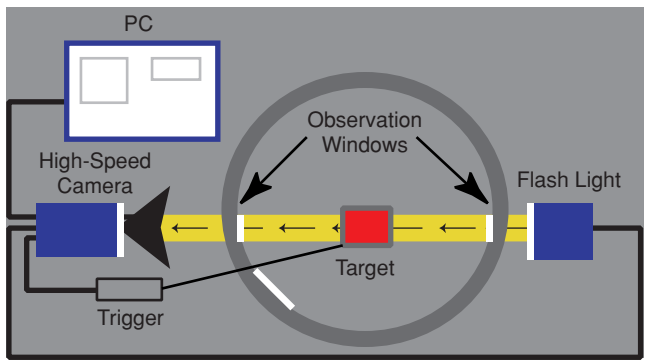

Fig.4 Shadowgraph system for optical observation

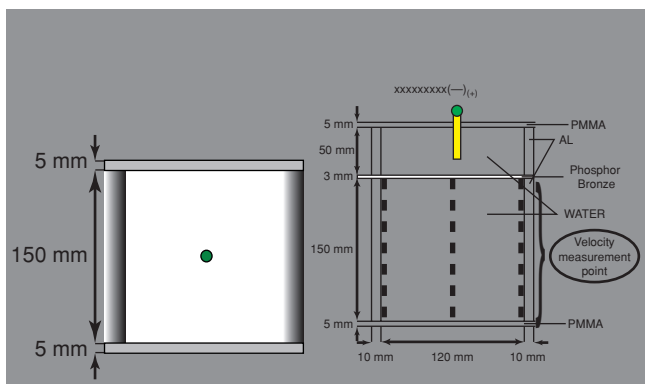

Fig.5 Schematic illustration of an optical observation for the framing photography.

device are PMMA. This container is separated into two parts by a phosphor bronze plate. One part is the shock wave generating container and the other is the food processing container. In order to generate a shock wave in the upper part of the device, the No.6 electric detonator (made by Kayaku Japan corporation) is set.

The inner volume of the shock wave generating container is 120 mm × 120 mm × 50 mm and the size of the food processing container is 120 mm × 120 mm × 150 mm. Water is poured into each.

2.2 NUMERICAL SIMULATION

The phenomenon for an explosion and the propagation of shock wave in the device are evaluated by means of LS-DYNA. Fig.6 shows to the numerical simulation model. This simulation model is two dimension model of one mesh in depth. And calculation method is used Lagrangian and Eulerian [3,4]. The number of elements is 29820 (=213 × 140 × 1).

High explosives SEP (made by Kayaku Japan corporation, detonation velocity about 6,800m/s, density 1310 kg/m^3) is detonated by using Initial detonation. Because the structure of the electric detonator is complex, SEP to which the parameter value is known instead of the electric detonator is used. We applied the constrained condition for the z axis so that a translational and rotational motion can not happen when explosion is occurred in explosive container.

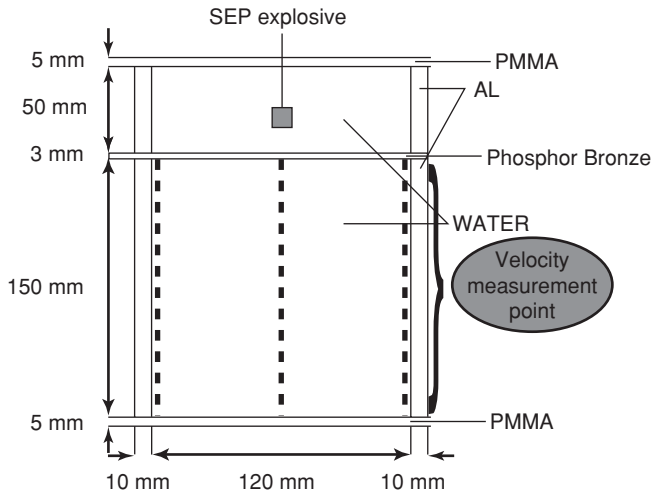

Fig.6 Numerical calculation model.

The various conditions used for this numerical simulation are shown below.

● Explosive SEP

Jones-Wilkins-Lee (JWL) equation of state [5,6] for the explosive SEP is used. This equation is well used for the numerical simulation accompanied by a detonation phenomenon. JWL parameters are given in Table 1. Expression of JWL equation of state is described as follows:

$$P = A\left[1-\frac{\omega}{VR_1}\right]\exp(-R_1V)+B\left[1-\frac{\omega}{VR_2}\right]\exp(-R_2V)+\frac{\omega E}{V} \tag{1}$$

$V = \rho_0$ (Initial density of an explosive)/ρ (Density of detonation gas), P is Pressure, E is Specific internal energy, A, B, R_1, R_2, ω are JWL parameters.

● WATER

We applied GRUNEISEN equation of state and NULL for the material parameter of water.

GRUNEISEN equation of state

This equation of state with cubic shock velocity-particle velocity defines pressure for compressed material as

$$p = \frac{\rho_0 C^2 \mu\left[1+\left(1-\frac{\gamma_0}{2}\right)\mu-\frac{a}{2}\mu^2\right]}{\left[1-(S_1-1)\mu-S_2\frac{\mu^2}{\mu+1}-S_3\frac{\mu^3}{(\mu+1)^2}\right]^2}+(\gamma_0+a\mu)E \tag{2}$$

C is the interceptof the $v_s - v_p$ curve, S_1, S_2 and S_3 are the coefficients of the slope of the $v_s - v_p$ curve, γ_0 is the Gruneisen gamma, a is the first order volume correction to γ_0, $\mu = \frac{\rho}{\rho_0} - 1$

Table 1 Parameter of JWL equation of state of SEP

	A [GPa]	**B [GPa]**	**R_1**	**R_2**	ω
SEP	364	2.31	4.3	1	0.28

Table 2 Parameter of Gruneisen equation of state of WATER

	c	S1	S_2	S_3	λ_0	a	E
WATER	1647.0	1.921	−0.096	0.0	0.35	0.0	2.895e+05

Gruneisen coefficients are given in Table 2.

NULL

This material allows equations of state to be considered without computing deviatoric stress. Optionally, a viscosity can be defined. Also, erosion in tension and compression is possible. Material parameter of WATER for NULL is given in Table 3.

- Aluminum alloy

We applied SIMPLIFIED JOHNSON COOK for the material parameter of Aluminum alloy. This Johnson cook strain sensitive plasticity is used for problems where the strain rates vary over a large range. In this simplified model, thermal effects and damage are ignored. The value of AL6082-T6 is used as a value of the aluminum alloy this time. Material parameter of Aluminum ally for SIMPLIFIED JOHNSON COOK are given in Table 4. Expression of SIMPLIFIED JOHNSON COOK is described as follows:

$$\sigma_y = (A + B\bar{\varepsilon}^{P^n})(1 + c\ln\varepsilon^*) \tag{3}$$

A, B, C and n are constants. $\bar{\varepsilon}^p$ = effective plastic strain. $\varepsilon^* = \frac{\dot{\bar{\varepsilon}}}{\dot{\varepsilon}_0}$ effective strain rate for $\dot{\varepsilon}_0 = 1s^{-1}$

- Phosphor bronze, PMMA

We applied PLASTIC KINEMATIC for the material parameter of Phosphor bronze and PMMA. This model is suited to model isotropic and kinematic hardening plasticity with option of including rate effects. Material parameter of Phosphor bronze and PMMA for PLASTIC KINEMATIC are given in Table 5.

- Coupling

In this research, CONSTRAINED LAGRANGE IN SOLID was used in order to perform coupling of water and metal material in LS-DYNA. This command provides the coupling mechanism for modeling Fluid-Structure Interaction (FSI). The structure can be constructed from Lagrangian shell and/or solid entities. The multi-material fluids are modeled by ALE formulation.

Other condition of numerical simulation is shown in Table 6.

Table 3 Material parameter of WATER

	RO	PC	MU	TEROD	CEROD	YM	PR
WATER	998.21002	0.0	8.684e-04	0.0	0.0	0.0	0.0

RO : Mass density PC : Pressure cutoff MU : Dynamic viscosity coefficient
TEROD,CEROD : Relative volume YM : Young's modulus PR : Poissin's ratio

Table 4 SIMPLIFIED JOHNSON COOK parameters of AL6082-T6

	A	B	C	n
AL6082-T6	4.285e + 08	3.277e + 08	0.00747	1.008

Table 5 Material parameters of phosphor bronze and PMMA

Phosphor bronze	RO	E	PR	SIGY	ETAN	BETA
	8890	1.2e + 11	0.38	6.0e + 08	0.0	0.0
	SRC	SRP	FS	VP		
	0.0	0.0	0.0	0.0		
PMMA	RO	E	PR	SIGY	ETAN	BETA
	1180	3.4e + 09	0.3	7.0e + 07	0.0	0.0
	SRC	SRP	FS	VP		
	0.0	0.0	0.0	0.0		

RO : Mass density E : Young's modulus PR : Poissin's ratio ETAN : Tangent modulus
BETA : Hardening parameter SRC : Strain rate parameter SRP : Strain rate parameter
FS : Failure strain eroding elements VP : Formulation for rate effects

Table 6 Condition of Numerical calculation analysis

Code	LS-DYNA	
Calculation method	Lagrangian & Eulerian	
Equation of state	SEP	JWL
	WATER	GRUNEISEN
MAT	WATER	NULL
	Aluminum alloy	SIMPLIFIED JOHNSON COOK
	PMMA	PLASTIC KINEMATIC
	Phosphor Bronze	PLASTIC KINEMATIC
Mesh size	1.0 × 1.0 × 1.0 mm	
Element	29820 (=213 × 140 × 1)	
Initial condition	INITIAL DETONATION	
Contact condition	ERODING SURFACE TO SURFACE	
Coupling condition	CONSTRAINED LAGRANGE IN SOLID	

3. RESULTS AND CONSIDERATION

3.1 EXPERIMENTAL RESULTS

The framing photographs showing the behavior of the shock wave which propagates the inside of a processing device were obtained by optical observation using the high-speed video camera. The framing photographs are shown in Fig.7. First, the shock wave with detonation velocity of No.6 electric detonator propagates into the water and the shock wave passes through the phosphor bronze plate at 5μs can be confirmed. The precursor shock wave generated by the shock wave propagated from the phosphor bronze plate to the aluminum sidewall can be confirmed at 20μs. It is understood that the precursor shock wave propagate from the phosphor bronze because the shock wave propagated from a lower wall before the shock wave reaches the upper wall. In the photograph of 35μs, the reflected wave that the shock wave that propagates by passing the phosphor bronze plate reflects to the sidewall was able to be observed. In addition, the height of the whole device is 213mm, but the distance from the phosphor bronze plate in the observation part is about 95mm at the maximum to observe the processing container part in the experiment.

From photographs of 20-30μs, the precursor shock wave that propagates into water from the aluminum sidewall of the device was able to be observed. Fig.8 shows the velocity

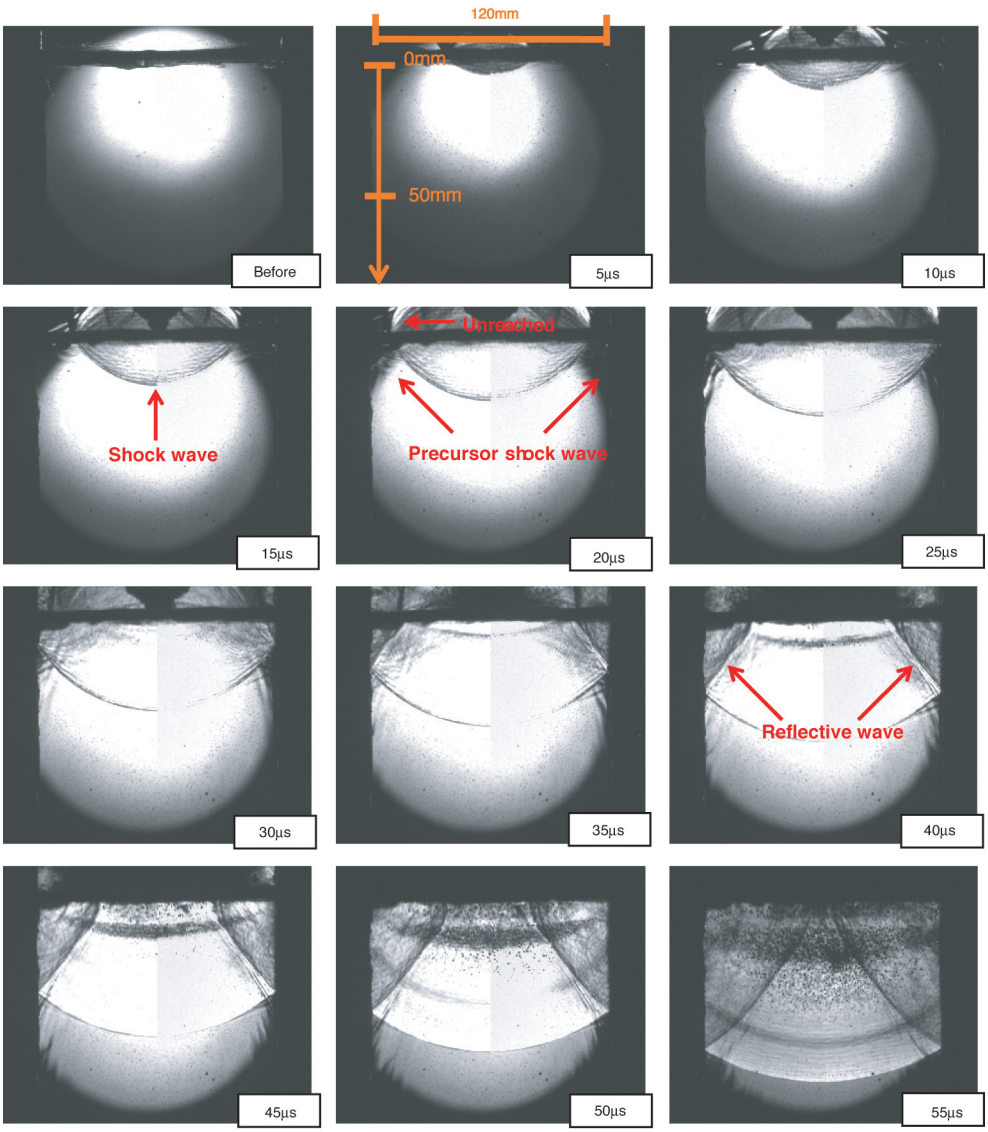

Fig.7 Framing photographs of underwater shock wave.

distribution of this precursor shock wave. The horizontal axis of this figure is a distance from the phosphor bronze plate. The velocity was measured along the aluminum sidewall in the photograph in Fig.7. It was confirmed that the velocity of precursor shock wave was decreased with passing times.

Fig.9 shows the velocity distribution of the first shock wave passes through the phosphor bronze plate in the center part of the figure. The horizontal axis of this figure is a distance from the phosphor bronze plate. The shock wave that propagated by passing the phosphor bronze plate was able to be observed in all photographs after the shock wave is generated. The velocity was measured in the center part in the photograph in Fig.7. The obtained velocity was about 1510m/s.

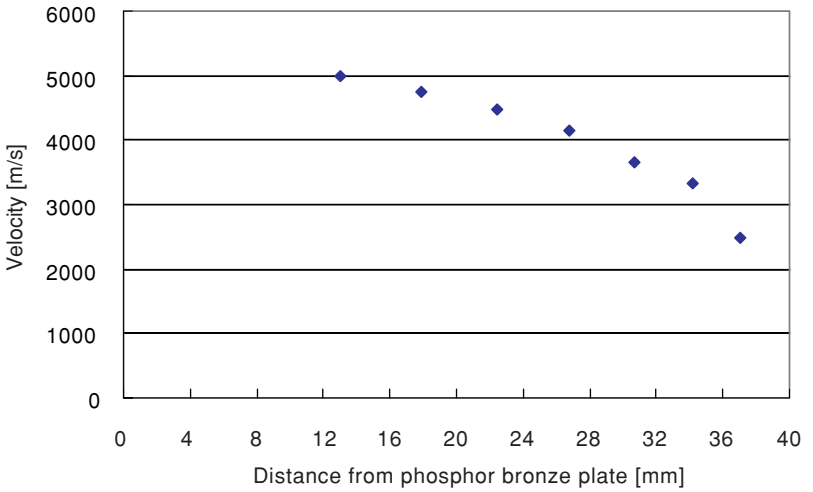

Fig.8 Velocity of precursor shock wave (optical observation).

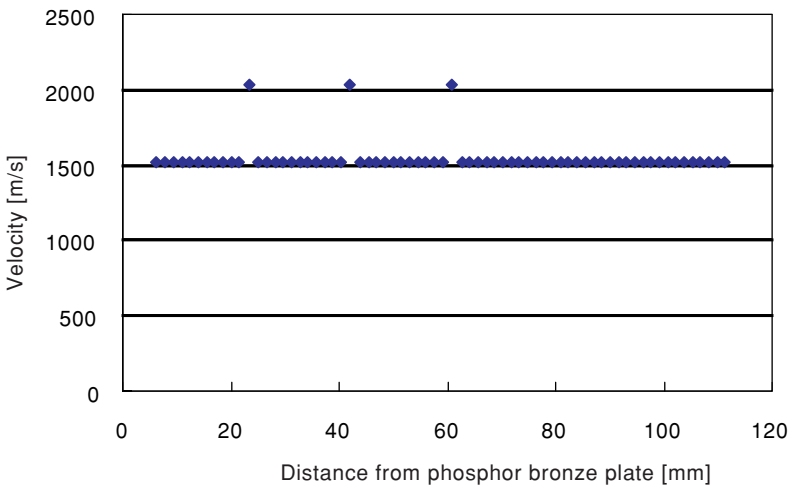

Fig.9 Velocity of shock wave (optical observation).

From the photograph after 35μs, the reflected shock wave that the shock wave that propagates by passing the phosphor bronze plate reflects to the sidewall was able to be observed. Fig.10 shows the velocity distribution of this reflected shock wave. The horizontal axis of this figure is a distance from the phosphor bronze plate. The velocity was measured along the aluminum sidewall in the photograph in Fig.7. It is understood that the reflected shock wave is gradually attenuate spread. At the point of about 80mm from the plate, it is converging on about 1500 m/s that is the sound velocity in water.

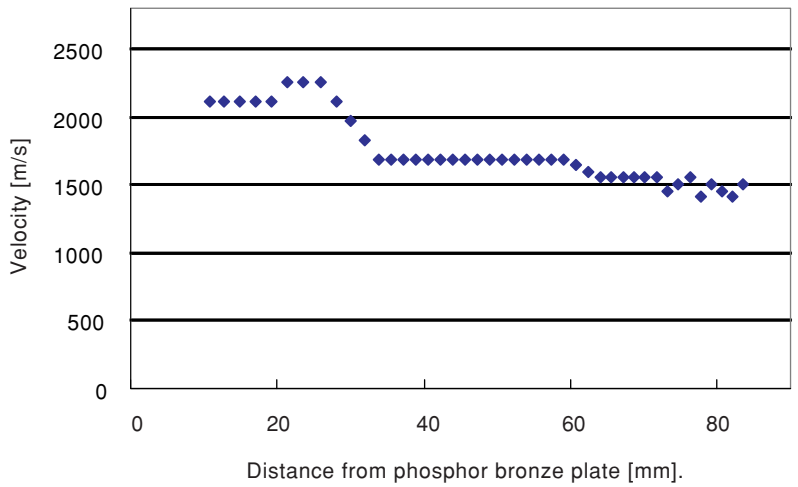

Fig.10 Velocity of reflective wave (optical observation).

3.2 NUMERICAL RESULTS

The pressure distribution of the precursor shock wave and the shock wave passes through the phosphor bronze plate that obtained by numerical simulation is shown in Fig.11. These photographs show that Explosive SEP explodes and shock wave propagates. The precursor shock wave propagates from the aluminum sidewall into water. Fig.12 has changed the pressure representation at the time of 60μs compared with Fig.11. The reflected shock wave that the shock wave that propagates by passing the phosphor bronze plate reflects to the sidewall was able to be observed.

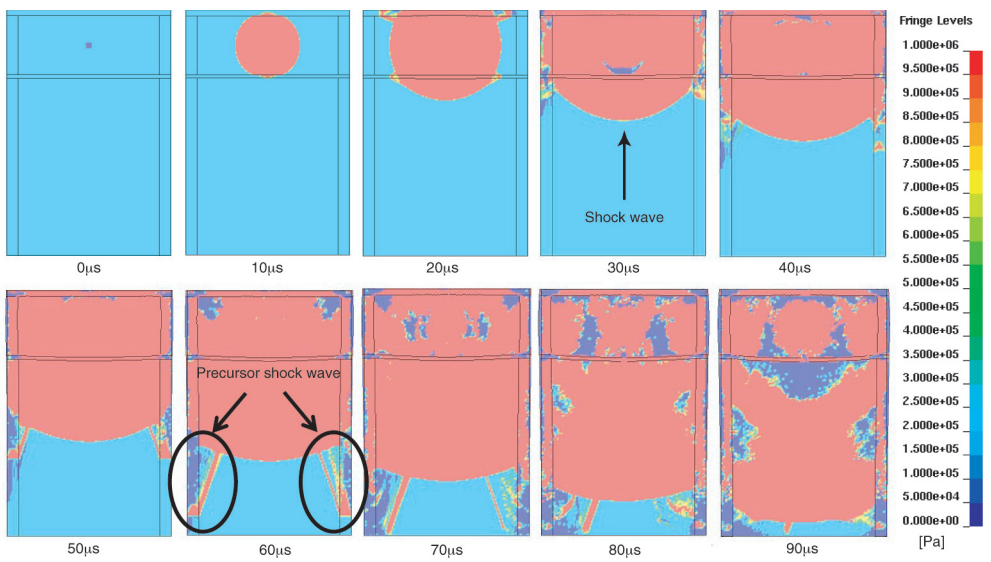

Fig.11 Calculated pressure contours under water (Precursor shock wave and shock wave).

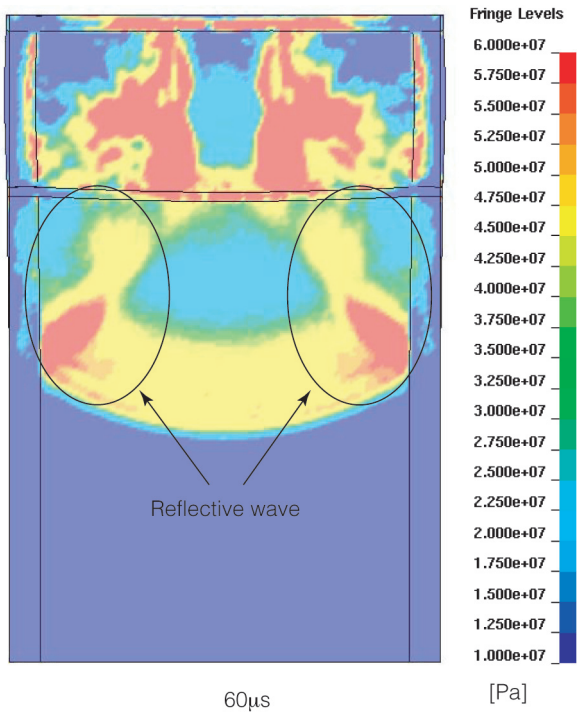

Fig.12 Calculated pressure contours under water (Reflective wave).

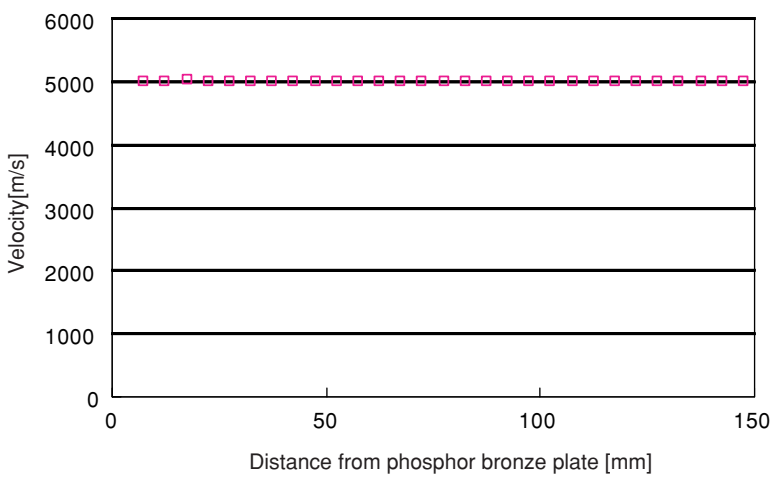

Fig.13 Velocity of precursor shock wave (numerical simulation).

From photographs of 30-80μs, the precursor shock wave that propagates into water from the aluminum sidewall of the device was able to be observed. Fig.13 shows the velocity distribution of this precursor shock wave. The horizontal axis of this figure is a distance from the phosphor bronze plate. The velocity was measured along the aluminum sidewall in the photograph in Fig.11.It is understood that the shock wave is advanced below with about 5000m/s.

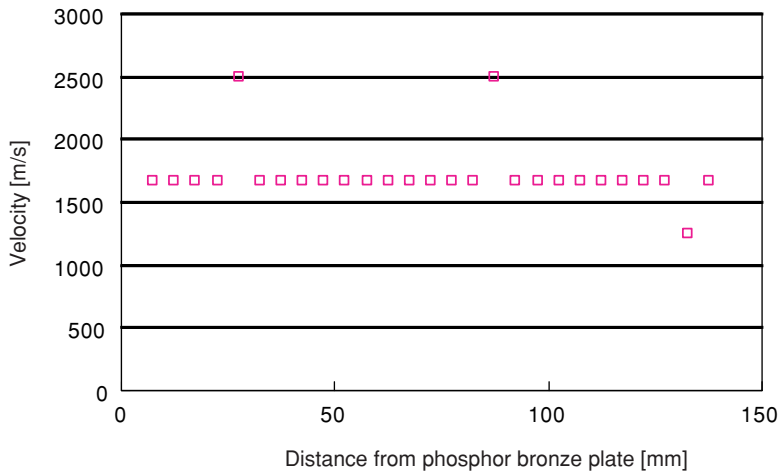

Fig.14 Velocity of shock wave (numerical simulation).

Fig.14 shows the velocity distribution of the shock wave passes through the phosphor bronze plate. The horizontal axis of this figure is a distance from the phosphor bronze plate. The velocity was measured in the center part in the photograph in Fig.11. The velocity doesn't attenuate and is about 1670m/s that is faster than the sound velocity in water.

The reflected shock wave shown in Fig.12 was able to be confirmed since 35μs. Fig.15 shows the velocity distribution of the reflected shock wave obtained since 35μs. The horizontal axis of this figure is a distance from the phosphor bronze plate. The velocity was measured along the aluminum sidewall in the photograph in Fig.12. The velocity that is about 2500m/s in 35μs attenuates gradually, and approaches the sound velocity in water from the plate in about 130mm.

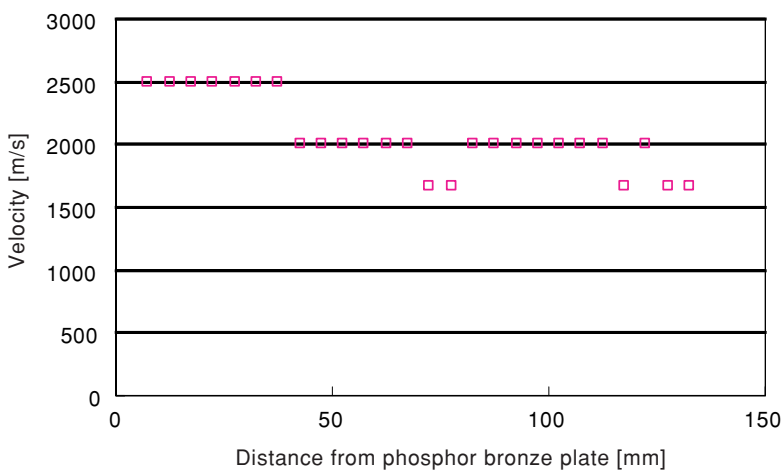

Fig.15 Velocity of reflective wave (numerical simulation)

3.3 COMPARISON OF RESULTS

What measured the velocity of precursor shock wave, shock wave passes through the phosphor bronze plate and shock wave reflected in the side wall is shown in Fig.16, Fig.17, and Fig.18.

- Precursor shock wave
  The velocity of shock wave at the time of the measurement start is approximately equal. However, it turns out that the precursor shock wave is attenuated in the experimental result and is not attenuated in the numerical simulation.

  In the experiment, the precursor shock wave attenuated rapidly, and the shape was not able to be judged clearly. Because it is considered that the shock wave (about 3000m/s) that propagated in PMMA on the observation side was observed.

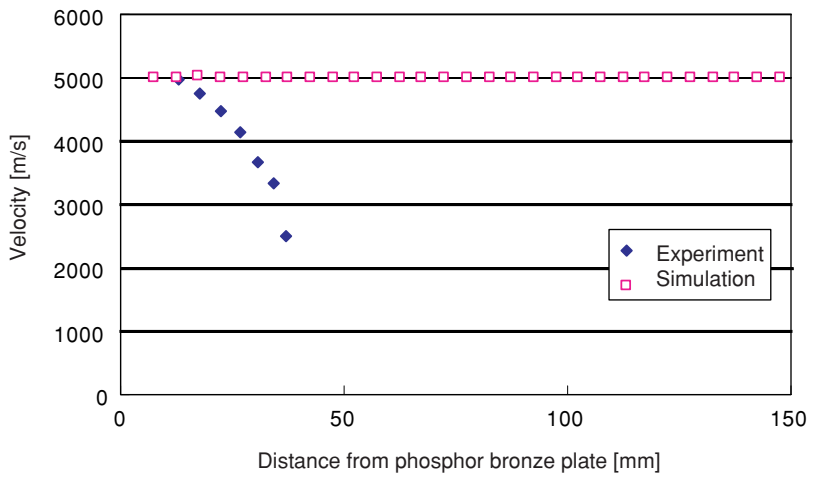

Fig.16 Comparison of velocity of precursor shock wave.

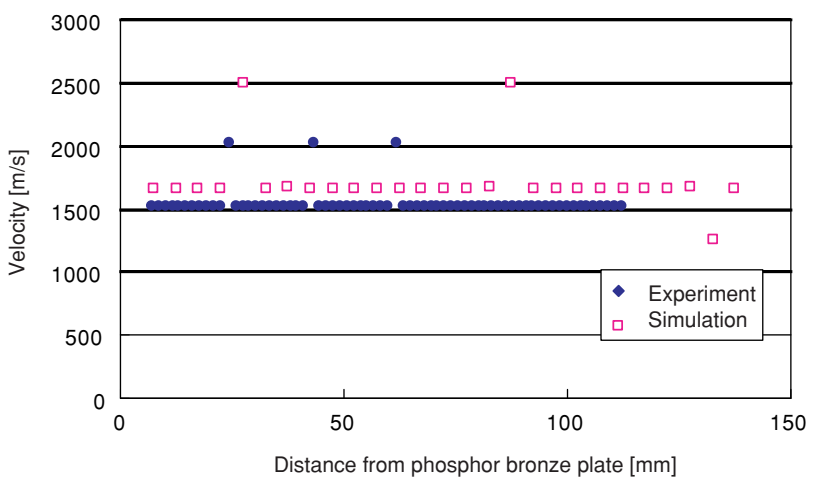

Fig.17 Comparison of velocity of shock wave.

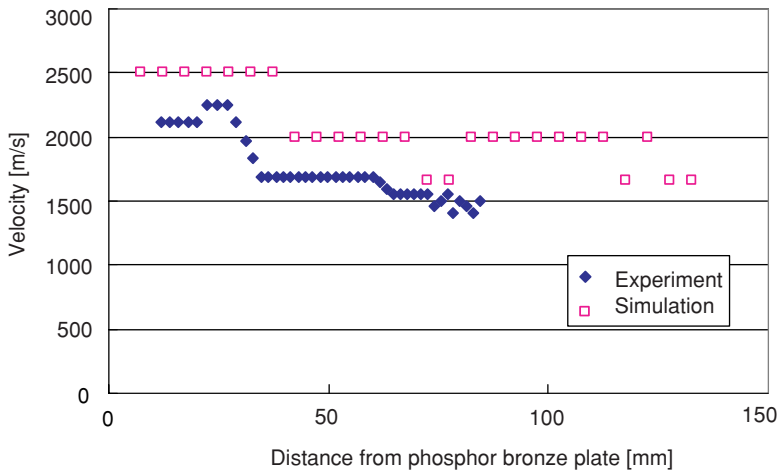

Fig.18 Comparison of velocity of reflective wave.

- Shock wave passes through the phosphor bronze plate
  The velocity of the shock wave did not attenuate and propagated into the water at a constant velocity in both results. In addition, the error by measurement also appeared. In general, it is known to settle the underwater shock wave to about 1500m/s. In this case, shock wave velocity propagated by about 1510 m/s in the experiment and propagated by about 1670 m/s in the numerical simulation. The cause that velocity is large in numerical simulation is considered that model is two dimensions.
- Shock wave reflected from the aluminum sidewall
  The shock wave velocity of the numerical simulation is faster than that of the experiment as well as the precursor shock wave, but it tends to attenuate gradually in both results. Although the velocity attenuates to the sound velocity in water (about 1500m/s) in the experiment, Fig.15 shows that the velocity is attenuate to about 1670m/s in the numerical results near 140mm from the plate that is the edge of the device in the numerical results.

The following are considered as the overall consideration of this experiment and the numerical analysis.

- The velocity of shock wave can not be measured accuracy since the photography interval of high - speed video camera is as large as 1μs.
- The attenuation of the velocity is smaller than an actual phenomenon because two dimension model is used, and the value with higher has gone out as a result in numerical simulation.
- The errors are caused by parameters of aluminum alloy, phosphor bronze, PMMA and water or contact conditions of an interface of each material in numerical simulation.

However, since there is the same tendency as an experiment and numerical analysis in each shock wave, it can be considerd that this numerical analysis is effective as the evaluation method.

4. CONCLUSION

This research aimed to take the correspondence by comparing the experiment and the numerical analysis to make the food processing container for trial purposes by the numerical

analysis. In the optical observation experiment, the behavior of a precursor shock wave from the device wall, the shock wave passes through the phosphor bronze plate and the reflected shock wave in the aluminum sidewall was able to be clarified. It has been understood that the precursor shock wave and the reflected shock wave attenuates near about 1500m/s that is the sound velocity in water.

Moreover, there is a different point of the way and generating time of attenuation. However, when the numerical analysis was compared with the result of the optical observation, it was corresponding in the point of the maximum velocity of precursor shock wave, behavior of the shock wave passes through the phosphor bronze plate and attenuation of the reflected shock wave.

To obtain a better numerical analysis result, it is enumerated to examine the parameter and the contact condition of the material of the numerical analysis in detail and to analyze three dimension model.

REFERENCE

[1] M.Otsuka, Syougeki Daidenryu ni yori Hasseisita Suityuusyougekiha no Seigyo to sono Oyou ni Kannsuru Kennkyu (Research on control and its application of the underwater shock wave generated by shock large current), Kumamot University (2007).

[2] S.Itoh, Z.Liu, Y.Nadamitu, An Investigation on the Properties of Underwater Shock Waves Generated in Underwater Explosions of High Explosives, *Journal of Pressure Vessel Technology*, Vol.119, pp. 498-502 (1997).

[3] J.O. Hallquist, "LS-DYNA Theoretical Manual", Livermore Software Technology Corporation (2006).

[4] J.O. Hallquist, "LS-DYNA Keyword User's Manual", Livermore Software Technology Corporation (2007).

[5] J. W. Kury, H. C.Hornig, E. L. Lee, J. L. McDonnel, D. L. Ornellas, M.Finger, F. M. Strange and M. L. Wilkins, Metal Acceleration by Chemical Explosives, 4th Symposium on Detonation, A109-A120 (1965).

[6] E. L. Lee, M.Finger and W.Collins, JWL Equation of state Coefficients for High Explosives, Lawrence Livermore Laboratory, UCID-16189 (1973).